AN ANALYTICAL COMPARISON OF THE ACOUSTIC ANALOGY AND KIRCHHOFF FORMULATION FOR MOVING SURFACES*

Kenneth S. Brentner and F. Farassat
NASA Langley Research Center Hampton, VA 23681

Abstract

The Lighthill acoustic analogy, as embodied in the Ffowcs Williams–Hawkings (FW–H) equation, is compared with the Kirchhoff formulation for moving surfaces. A comparison of the two governing equations reveals that the primary advantage of the Kirchhoff formulation (namely that nonlinear flow effects are included in the surface integration) is also available to the FW–H method if the integration surface used in the FW–H equation is not assumed to be impenetrable. The FW–H equation is analytically superior for aeroacoustics because it is based on the conservation laws of fluid mechanics rather than on the wave equation. Thus, the FW–H equation is valid even if the integration surface is in the nonlinear region. This advantage is demonstrated numerically. With the Kirchhoff approach, substantial errors can result if the integration surface is not positioned in the linear region, and these errors may be hard to identify. Finally, new metrics, based on the Sobolev norm, are introduced that may be used to compare input data for both quadrupole noise calculations and Kirchhoff noise predictions.

Nomenclature

c = sound speed in quiescent medium
dS = element of the integration surface area
$f = 0$ = function that describes the integration surface
$H(f)$ = Heaviside function, $H(f) = 0$ for $f < 0$ and $H(f) = 1$ for $f > 0$
L_M = $L_i M_i$
L_i = components of vector defined in Eq. (15)
L_r = $L_i \hat{r}_i$
$\dot{L}_r$ = $\dot{L}_i \hat{r}_i$
$\mathbf{M}$ = local Mach number vector of source, with components M_i
M = $|\mathbf{M}|$
M_{AT} = advancing-tip Mach number
M_H = hover tip Mach number
M_n = Mach number of source in direction normal to source surface, $M_i \hat{n}_i$
M_r = Mach number of source in radiation direction, $M_i \hat{r}_i$
$\dot{M}_r$ = $\dot{M}_i \hat{r}_i$
$\hat{\mathbf{n}}$ = unit outward normal vector to surface, with components $\hat{n}_i$
P_{ij} = compressive stress tensor with constant $p_o \delta_{ij}$ subtracted
p = pressure
p' = acoustic pressure, $p - p_o$ outside source region $p' \equiv c^2 \rho'$ on the left-hand side of FW–H and Kirchhoff equations
Q_{KIR} = symbol for Kirchhoff equation source terms defined in Eq. (8)
R = rotor radius
r = distance between observer and source, $r = |\mathbf{x} - \mathbf{y}|$
$\hat{\mathbf{r}}$ = unit vector in the radiation direction, with components $\hat{r}_i$; $\hat{\mathbf{r}} = (\mathbf{x} - \mathbf{y})/r$
T_{ij} = Lighthill stress tensor, $\rho u_i u_j + P_{ij} - c^2 \rho' \delta_{ij}$
t = observer time

*Presented at the American Helicopter Society 53rd Annual Forum, Virginia Beach, VA, April 29–May 1, 1997. This revision of the paper is published in the *AIAA Journal*, Vol. 36, No. 8, August 1998, pp. 1379–1386.

U_i = components of vector defined in Eq. (14)
U_n = $U_i \hat{n}_i$
$\dot{U}_n$ = $\dot{U}_i \hat{n}_i$
$U_{\dot{n}}$ = $U_i \dot{\hat{n}}_i$
u_i = components of local fluid velocity
u_n = $u_i \hat{n}_i$
v_n = local normal velocity of source surface
$\mathbf{x}$ = observer position vector, with components x_i
$\mathbf{y}$ = source position vector, with components y_i
$\delta(f)$ = Dirac delta function
δ_{ij} = Kronecker delta, $\delta_{ij} = 1$ for $i = j$, otherwise $\delta_{ij} = 0$
μ = advance ratio
ρ = density of fluid
ρ' = density perturbation, $\rho - \rho_o$
τ = source time
$\Box^2$ = wave operator, $\Box^2 \equiv \dfrac{1}{c^2}\dfrac{\partial^2}{\partial t^2} - \nabla^2$

Subscripts:
L = loading noise component
o = fluid variable in quiescent medium
Q = quadrupole noise component
ret = quantity evaluated at retarded time, $\tau = t - r/c$
T = thickness noise component

Note: Summation convention is used in this paper when vector or tensor components have indices i and j. A dot over a symbol indicates source-time differentiation, $\partial/\partial\tau$.

Introduction

A great deal of progress has been made in recent years in the prediction of rotating-blade noise through methods that utilize first principles. Several reasons account for this progress. First, a detailed and fundamental understanding of how rotor blades generate noise has been gained through several acoustic wind-tunnel and flight tests. Secondly, a rigorous theoretical basis for predicting the noise that is generated by rotating blades has been developed. In fact, several prediction methodologies with a solid physical and mathematical basis are currently available: formulations based upon the Lighthill acoustic analogy [1] (in particular, the Ffowcs Williams and Hawkings (FW–H) equation [2]) and the Kirchhoff formulations for both subsonic and supersonic moving surfaces [3, 4].

In their 1969 paper, Ffowcs Williams and Hawkings [2] utilized the powerful technique of generalized function theory to develop both the equation that has become associated with their names and the governing equation of the Kirchhoff formulation for moving surfaces. The FW–H equation is an exact rearrangement of the continuity equation and the Navier–Stokes equations into the form of an inhomogeneous wave equation with two surface source terms (monopole and dipole) and a volume source term (quadrupole). Although the quadrupole source contribution is insignificant in many subsonic applications, substantially more computational resources are needed for volume integration when the quadrupole source is required. The expression of the aeroacoustic noise problem as a Kirchhoff problem received little attention for many years because the method of deriving the FW–H equation is efficient and physically illuminating. The governing equation of the Kirchhoff formulation for moving surfaces is an inhomogeneous wave equation in which the sources are distributed on a fictitious surface (i.e., the Kirchhoff surface) which encloses all of the physical sources. The Kirchhoff formulation is attractive because no volume integration is necessary. Until recently, the source strength information on the Kirchhoff surface was not readily available for problems of aeroacoustic significance because the discipline of computational fluid dynamics (CFD) was not mature enough. Today, both the FW–H and Kirchhoff methods are viable alternatives for the aeroacoustic noise problem.

Although the availability of more than one formulation for predicting noise is useful, no clear consensus exists on which method to choose for a particular application. Recently, Brentner et al. [5] compared the helicopter rotor noise prediction code WOPWOP+ [6–8], which uses a FW–H based formulation that

includes an approximate quadrupole calculation, with a rotating Kirchhoff code RKIR [9, 10]; this study showed that both methods *can* predict the rotor noise equally well. In that work, however, neither method was demonstrated to be clearly superior. It was di Francescantonio [11] who first to demonstrated that for far-field helicopter rotor noise prediction the FW–H approach can be used on a fictitious surface that does not correspond to a physical body—exactly like the Kirchhoff approach. Reference 11 demonstrates that when the FW–H approach is applied on a Kirchhoff-type surface that the quadrupole sources enclosed by the surface are accounted for by the surface sources. Furthermore, di Francescantonio concludes that a main advantage to using the FW–H approach over the Kirchhoff approach is that the FW–H method does not require a knowledge of $\partial p/\partial n$ (which can be troublesome to compute) on the integration surface. Nevertheless, no clear advantage to using the FW–H method over the Kirchhoff method is evident in di Francescantonio's numerical comparisons. Pilon and Lyrintzis [12] also tried to explain the relationship between the FW–H and Kirchhoff methods and derived a form of the FW–H equation that can be utilized like a Kirchhoff method; however, their results are difficult to follow and ambiguous.

Dissatisfaction with the previous attempts to explain the relationship between the FW–H and Kirchhoff approaches has lead to the main purpose of this paper: to analytically compare these two acoustic prediction methodologies and to reduce the general confusion that currently exists among potential aeroacoustic formulation users about the relationship between the two methods. This purpose necessarily includes a comparison of how the governing equations are derived, with the differences in the derivations highlighted. Both analytical and numerical comparisons are utilized to determine whether one method has a clear advantage over the other in terms of efficiency, accuracy, and robustness. Finally, a useful metric for comparing formulations is outlined.

Advantages and Disadvantages

First, the advantages and disadvantages of both the FW–H and Kirchhoff formulations must be considered in order to understand the motivation for a more in-depth analysis.

FW–H

Approach

The FW–H approach has several advantages over the Kirchhoff method. First, the three source terms in the FW–H equation each have physical meaning, which is helpful in understanding the noise generation. The thickness noise (monopole source) is determined completely by the geometry and kinematics of the body. The loading noise (dipole source) is generated by the force that acts on the fluid as a result of the presence of the body. The classification of thickness and loading noise is related to the thickness and loading problems of linearized aerodynamics. Thus, this terminology is consistent with that of aerodynamics. The quadrupole source term accounts for nonlinear effects (e.g., nonlinear wave propagation and steepening; variations in the local sound speed; and noise generated by shocks, vorticity, and turbulence in the flow field) [13–15].

All three source terms are interdependent, yet their physical basis provides information that can be used to design quieter rotors. The separation of the source terms also is an advantage numerically because not all terms must be computed at all times if a particular source does not contribute to the sound field (e.g., for low-speed flow, the quadrupole source term may be neglected; in the rotor plane, thickness noise is dominant). A final advantage of FW–H-based computer codes is that these codes are relatively mature and have robust numerical algorithms that have been validated for many aeroacoustic problems of industrial interest. These same numerical algorithms may encounter new difficulties when applied to Kirchhoff-type integration surfaces because the variation in retarded time is substantially greater over a large surface and the individual panel size can also be significantly larger. The main disadvantage of the traditional application in the FW–H method is that to predict the noise of bodies moving at transonic speeds the quadrupole source must be included. Thus, the quadrupole—which is a volume source—ultimately requires a volume integration of the entire source region. Volume integration is computationally expensive and can be difficult to implement. Although the computational effort can be reduced by approximating the quadrupole [7, 8], it cannot be avoided completely. This problem is not unique to rotor calculations.

Kirchhoff Approach

The Kirchhoff approach does not require volume integration because it has only surface source terms. Hence, the Kirchhoff method has been used for the past few years in the prediction of transonic rotor noise. Unlike the FW–H source terms, however, the Kirchhoff source terms are not easily related to thickness,

loading, nonlinear effects, or indeed any physical mechanisms. The Kirchhoff source terms provide little guidance for design. Another disadvantage of the Kirchhoff method is that the Kirchhoff surface must be chosen to be in the *linear flow region*, such that the input acoustic pressure $p' \equiv p - p_o$ and its derivatives $\partial p'/\partial t$ and $\partial p'/\partial n$ are compatible with the wave equation. The location of the linear region is not well defined and is problem dependent. Ideally, the Kirchhoff surface should be placed well away from the source region, but CFD solutions typically are not as well resolved or as accurate away from the body. Hence, the placement of the Kirchhoff surface is usually a compromise.

Analytical Comparison

Now that the general characteristics of both the FW–H and Kirchhoff formulations have been described, a more detailed comparison is presented. First, we consider the development of the governing equations of both approaches to gain insight into the validity of each formulation. Then, an assessment of an integral formulation for subsonic source motion is provided.

Governing Equations

FW–H

Equation

The FW–H equation [2] is the most general form of the Lighthill acoustic analogy and is appropriate for predicting the noise generated by the complex motion of helicopter rotors. The FW–H equation can be derived by embedding the exterior flow problem in unbounded space by using generalized functions to describe the flow field. Consider a moving surface $f(\mathbf{x}, t) = 0$ with a stationary fluid outside. The surface $f = 0$ is defined such that $\nabla f = \hat{\mathbf{n}}$, where $\hat{\mathbf{n}}$ is a unit normal vector that points into the fluid. Inside $f = 0$, the generalized flow variables are defined as having their free-stream values; that is

$$\tilde{\rho} = \begin{cases} \rho & f > 0 \\ \rho_o & f < 0 \end{cases} \tag{1}$$

$$\widetilde{\rho u_i} = \begin{cases} \rho u_i & f > 0 \\ 0 & f < 0 \end{cases} \tag{2}$$

and

$$\widetilde{P}_{ij} = \begin{cases} P_{ij} & f > 0 \\ 0 & f < 0 \end{cases} \tag{3}$$

where the tilde indicates that the variable is a generalized function defined throughout all space. On the right side, ρ, ρu_i, and P_{ij} are the density, the momentum, and the compressive stress tensor, respectively. Note that we have absorbed the constant $-p_o\delta_{ij}$ into the definition of P_{ij} for convenience; hence, for an inviscid fluid, $P_{ij} = p'\delta_{ij}$. Free-stream quantities are indicated by the subscript o, and δ_{ij} is the Kronecker delta.

By using definitions of Eqs. (1)–(3), a generalized continuity equation can be written as

$$\frac{\bar{\partial}\tilde{\rho}}{\partial t} + \frac{\bar{\partial}\widetilde{\rho u_i}}{\partial x_i} = (\rho' \frac{\partial f}{\partial t} + \rho u_i \frac{\partial f}{\partial x_i})\delta(f) \tag{4}$$

where the bar over the derivative operators indicates that generalized differentiation (i.e., differentiation of generalized functions) is implied and $\rho' \equiv \rho - \rho_o$. Also note that $\partial f/\partial t = -v_n$, $\partial f/\partial x_i = \hat{n}_i$, and $\delta(f)$ is the Dirac delta function. This generalized continuity equation is valid for the entire space, both inside and outside the body. The generalized momentum equation can be written as

$$\frac{\bar{\partial}\widetilde{\rho u_i}}{\partial t} + \frac{\bar{\partial}\widetilde{\rho u_i u_j}}{\partial x_j} + \frac{\bar{\partial}\tilde{P}_{ij}}{\partial x_j} = \left[\rho u_i \frac{\partial f}{\partial t} + (\rho u_i u_j + P_{ij}) \frac{\partial f}{\partial x_j}\right]\delta(f) \ . \tag{5}$$

Now if we take the time derivative of Eq. (4), subtract the divergence of Eq. (5), and then rearrange terms, the FW–H equation can be written as the following inhomogeneous wave equation:

$$\begin{aligned}\Box^2 p'(\mathbf{x},t) = & \frac{\bar{\partial}^2}{\partial x_i \partial x_j}\{T_{ij}H(f)\} \\ & - \frac{\partial}{\partial x_i}\Big\{[P_{ij}\hat{n}_j + \rho u_i(u_n - v_n)]\delta(f)\Big\} \\ & + \frac{\partial}{\partial t}\Big\{[\rho_o v_n + \rho(u_n - v_n)]\delta(f)\Big\} \end{aligned} \tag{6}$$

where T_{ij} is the Lighthill stress tensor, u_n is the fluid velocity in the direction normal to the surface $f = 0$, and v_n is the surface velocity in the direction normal to the surface. On the left side we use the customary notation $p' \equiv c^2\rho'$ because the observer location is outside the source region. In this derivation, we follow the mathematical procedure for deriving the FW–H equation given by Farassat [16].

Often in the derivation of the FW–H equation, the surface $f = 0$ is assumed to be both coincident with the physical body surface and impenetrable ($u_n = v_n$). That assumption is not necessary and has not been made in Eq. (6) so that the equation may be compared more directly with the governing equation of the Kirchhoff formula for moving surfaces. Ffowcs Williams and Hawkings used slightly different mathematical manipulations [2], but clearly they understood that choosing the integration surface coincident with the physical body was not necessary (even though Ref. 2 was dealing with *physical* surfaces). Ffowcs Williams presented Eq. (6) in various references (e.g., section 9.2 in Ref. 17 and section 11.10 in Ref. 18) and described several possible implications of a permeable surface $f = 0$ in section 11.10 of Ref. 18. Recently, di Francescantonio [11]—apparently unaware of Ffowcs Williams work—rederived Eq. (6) with essentially the same method as presented here calling it the KFWH (Kirchhoff—FW–H) formula to emphasize the fact the he used a surface $f = 0$ which was off the body and permeable. Pilon and Lyrintzis [12] also treated the FW–H on a permeable surface calling it an improved Kirchhoff method. (The results of Pilon and Lyrintzis are ambiguous because the substitution $p' = c^2\rho'$ was made in three source terms without explanation (Eq. (11), Ref. 12). Although this substitution is correct if p' is *defined* as $c^2\rho'$, we believe this ambiguity will lead to confusion and errors in practice.) We prefer to continue to refer to Eq. (6) as the FW–H equation, rather than the KFWH or improved Kirchhoff method, because Ffowcs Williams published it first.

Kirchhoff Equation

The development of the Kirchhoff formulation utilizes the same mathematical style and rigor as used in the derivation of the FW–H equation. The difference is that the domain is now considered in terms of wave propagation. The surface $f = 0$ is defined such that the acoustic sources are contained inside the surface. Then, the acoustic pressure $p'(\mathbf{x},t)$ (or any other variable) is extended such that

$$\widetilde{p'} = \begin{cases} p' & f > 0 \\ 0 & f < 0 \end{cases} \tag{7}$$

and the generalized wave equation—which is the governing equation for the Kirchhoff formulation—becomes

$$\begin{aligned}\Box^2 p'(\mathbf{x},t) = & -\Big(\frac{\partial p'}{\partial t}\frac{M_n}{c} + \frac{\partial p'}{\partial n}\Big)\delta(f) \\ & - \frac{\partial}{\partial t}\Big[p'\frac{M_n}{c}\delta(f)\Big] - \frac{\partial}{\partial x_i}\Big[p'\hat{n}_i\delta(f)\Big] \\ \equiv & \; Q_{\mathrm{KIR}} \end{aligned} \tag{8}$$

where $M_n = v_n/c$. Ffowcs Williams and Hawkings derived this equation in Ref. 2. In this equation, p' must be compatible with the wave equation (i.e., a solution of the wave equation on $f = 0$); hence, Eq. (8) is valid only in the region of the fluid in which the wave equation is the appropriate governing equation. (See Farassat and Myers [3, 4] for more details.)

Source Term Comparison

It is well known that the wave equation can be derived directly from the conservation laws of fluid mechanics; however, our objective in this paper is to show how Eq. (8) is related to the FW–H equation

(Eq. (6)). To that end, we add and subtract terms to the inviscid form of Eq. (6) to manipulate the source terms into the form of Eq. (8). This manipulation yields

$$\begin{aligned}\Box^2 p'(\mathbf{x},t) = Q_{\mathrm{KIR}} + \; & \frac{\bar{\partial}^2}{\partial x_i \partial x_j}[T_{ij}H(f)] \\ + \; & \big(\frac{\partial p'}{\partial t}\frac{M_n}{c} + \frac{\partial p'}{\partial n}\big)\delta(f) + \frac{\partial}{\partial t}\big[(p' - c^2\rho')\frac{M_n}{c}\delta(f)\big] \\ - \; & \frac{\partial}{\partial x_i}\big[\rho u_i(u_n - v_n)\delta(f)\big] + \frac{\partial}{\partial t}\big[\rho u_n \delta(f)\big] \; . \end{aligned} \tag{9}$$

If we note that

$$\frac{\bar{\partial}^2 H(f)}{\partial t \partial x_i} = \frac{\partial}{\partial t}\Big[\hat{n}_i \delta(f)\Big] = -\frac{\partial}{\partial x_i}\Big[v_n \delta(f)\Big] \tag{10}$$

and utilize the continuity and momentum equations, then we can rewrite Eq. (9) as

$$\begin{aligned}\Box^2 p'(\mathbf{x},t) = Q_{\mathrm{KIR}} + \; & \frac{\bar{\partial}^2}{\partial x_i \partial x_j}\big[T_{ij}H(f)\big] \\ + \; & \frac{\partial}{\partial t}\big[p' - c^2\rho'\big]\frac{M_n}{c}\delta(f) + \frac{\partial}{\partial t}\big[(p' - c^2\rho')\frac{M_n}{c}\delta(f)\big] \\ - \; & \frac{\partial}{\partial x_j}\big[\rho u_i u_j\big]\hat{n}_i\delta(f) - \frac{\partial}{\partial x_i}\big[\rho u_i u_n \delta(f)\big] \; . \end{aligned} \tag{11}$$

This form of the FW–H equation is useful because the source terms that are not found in the Kirchhoff governing equation can be easily identified. This form of the FW–H equation is an important new result of this paper. The additional source terms not included in the Kirchhoff governing equation are second order and may be neglected in the linear flow region. This result was precisely Lighthill's original premise—the wave equation is the appropriate governing equation outside a limited source region. In fact, when $p' = c^2\rho'$, Eq. (11) becomes

$$\Box^2 p'(\mathbf{x},t) = Q_{\mathrm{KIR}} + \; \frac{\bar{\partial}^2 \rho u_i u_j}{\partial x_i \partial x_j} H(f) \; . \tag{12}$$

Notice that the Heaviside function has been taken out of the quadrupole source term of Eq. (11) in the manipulations that lead to Eq. (12). The only remaining source term that is not in Eq. (8) is clearly second order in the perturbation quantity u_i. This term would be neglected in the derivation of the wave equation from the fluid conservation laws. Hence, we show that the FW–H and Kirchhoff formulations are indeed equivalent when the integration surface is placed in the linear region of the flow (i.e., where the input data are compatible with the wave equation).

The FW–H equation and the Kirchhoff governing equation differ significantly, however, when the integration surface is in the source region. The implications of this difference are demonstrated later with numerical examples. If the FW–H equation integration surface is on the body or in the source region, the quadrupole—a volume source term—must be included to accurately predict the noise. Therefore, we can infer that as we move the integration surface of the FW–H equation away from the body the contribution of the volume quadrupole contained within the integration surface must now be accounted for by the surface source terms. This has been shown by di Francescantonio [11] to be the case for a hovering helicopter rotor. We provide a numerical demonstration later in the paper.

For completeness, Eq. (11) can be simplified by canceling terms and the rearranging; the result is

$$\begin{aligned}\Box^2 p'(\mathbf{x},t) = -\big(\frac{\partial c^2\rho'}{\partial t}\frac{M_n}{c} + \frac{\partial \rho u_i}{\partial t}\hat{n}_i\big)\delta(f) \\ - \frac{\partial}{\partial t}\big[c^2\rho'\frac{M_n}{c}\delta(f)\big] - \frac{\partial}{\partial x_i}\big[(p'\hat{n}_i + \rho u_i u_n)\delta(f)\big] \\ + \; \frac{\partial^2}{\partial x_i \partial x_j}\big[T_{ij}H(f)\big] \; . \end{aligned} \tag{13}$$

Notice that the surface source terms in Eq. (13) are closely related to Eq. (8). In fact, by substituting $c^2\rho'$ for p' in the time derivative terms in Eq. (8) and $\rho u_i u_j + p'\delta_{ij}$ for p' in the spatial derivative terms we obtain the surface source terms in Eq. (13). (The momentum equation is used to exchange $\partial(\rho u_i u_j + p'\delta_{ij})/\partial x_j$ with $-\partial \rho u_i/\partial t$ in Eq. (13).) Although the relationship between Eq. (13) and Eq. (8) is interesting, Eq. (13) has two pitfalls: it is not easily recognized as the FW–H equation, and no clear connections can be made between the form of the source terms and the problem physics.

An Integral Formulation

Now that the relationship between the FW–H equation and the Kirchhoff formulation has been established at the governing equation level, we develop an applicable integral form that is appropriate for subsonic source motion. This form is needed for the ultimate implementation and numerical comparison of the different formulations.

Equation (6) is the appropriate form of the FW–H equation from which to develop an integral representation the the same form as the traditional application of the FW–H equation. A great simplification comes if we, following di Francescantonio [11], now define new variables U_i and L_i as

$$U_i = (1 - \frac{\rho}{\rho_o})v_i + \frac{\rho u_i}{\rho_o} \tag{14}$$

and

$$L_i = P_{ij}\hat{n}_j + \rho u_i(u_n - v_n) \ . \tag{15}$$

We have chosen slightly different but equivalent definitions from those in Ref. 11 because ρ and ρu_i are conservation variables that are often utilized in CFD codes. With these definitions, the FW–H equation may be written in its standard differential form as

$$\begin{aligned} \Box^2 p'(\mathbf{x},t) = & \frac{\partial^2}{\partial x_i \partial x_j}[T_{ij}H(f)] \\ & - \frac{\partial}{\partial x_i}[L_i\delta(f)] + \frac{\partial}{\partial t}[(\rho_o U_n)\delta(f)] \ . \end{aligned} \tag{16}$$

This equation is particularly useful because formulation 1A (due to Farassat [6,19]) can be utilized directly to write an integral representation of the solution as

$$p'(\mathbf{x},t) = p'_T(\mathbf{x},t) + p'_L(\mathbf{x},t) + p'_Q(\mathbf{x},t) \tag{17}$$

where

$$\begin{aligned} 4\pi p'_T(\mathbf{x},t) = & \int_{f=0} \Big[\frac{\rho_o(\dot{U}_n + U_{\dot{n}})}{r(1-M_r)^2}\Big]_{ret} dS \\ & + \int_{f=0} \Big[\frac{\rho_o U_n(r\dot{M}_r + c(M_r - M^2))}{r^2(1-M_r)^3}\Big]_{ret} dS \quad , \end{aligned} \tag{17a}$$

$$\begin{aligned} 4\pi p'_L(\mathbf{x},t) = & \frac{1}{c}\int_{f=0} \Big[\frac{\dot{L}_r}{r(1-M_r)^2}\Big]_{ret} dS \\ & + \int_{f=0} \Big[\frac{L_r - L_M}{r^2(1-M_r)^2}\Big]_{ret} dS \\ & + \frac{1}{c}\int_{f=0} \Big[\frac{L_r(r\dot{M}_r + c(M_r - M^2))}{r^2(1-M_r)^3}\Big]_{ret} dS \quad , \end{aligned} \tag{17b}$$

and $p'_Q(\mathbf{x},t)$ can be determined by any method that is currently available. (Ref. 8 gives an approximate quadrupole formulation; Refs. 19 and 6 give the derivation of Eqs. (17a) and (17b).) In Eq. (17), the

dot over a variable implies source-time differentiation of that variable, $L_M = L_i M_i$, and a subscript r or n indicates a dot product of the vector with the unit vector in the radiation direction $\hat{\mathbf{r}}$ or the unit vector in the surface normal direction $\hat{\mathbf{n}}$, respectively.

Current rotor noise prediction codes can easily be modified to accommodate this new implementation of the FW–H equation. The major difference is that the integration surface is no longer restricted to the rotor blade surface, and in addition to p' the values of ρ and ρu_i are needed as input. When the integration surface *does* correspond to the blade surface, the separation of source terms into thickness, loading, and quadrupole noise still has physical meaning; otherwise, the separation of the source terms into p'_T, p'_L, and p'_Q is only mathematical. Hence, the ability to give physical interpretation to the source terms continues to be a distinct and unique advantage of the FW–H equation.

Numerical Comparison of Formulations

Although we have shown analytically that the FW–H formulation has advantages over the Kirchhoff formulation, the deciding factor is how these methods compare in practice. Some comparisons have already been made (e.g., Refs. 5, 11, and 20). In Ref. 11, di Francescantonio concludes that a main advantage to applying the FW–H equation on a Kirchhoff-type integration surface is that interaction with CFD codes is easier because the normal derivative of pressure is no longer required. If this were the only advantage (indeed we recognize that the normal derivative calculation can be cumbersome), then a simple solution would be to make the substitution

$$\frac{\partial p}{\partial n} = -\hat{n}_i \frac{\partial \rho u_i}{\partial t} \tag{18}$$

in Eq. (8). This result is simply the linear normal momentum equation, which is applicable in the linear flow region. Nevertheless, we have identified other advantages that we now demonstrate numerically.

For this work, the RKIR code (rotating Kirchhoff formulation) originally developed by Lyrintzis et al. [10] has been extensively modified to test the numerical implementation of Eq. (17) without the quadrupole source term. We refer to the modified code as FW–H/RKIR here. The RKIR code was chosen as the platform to test the new FW–H implementation primarily because it already performs integration on a surface that is positioned some distance from the rotor blade and has been coupled to the full-potential flow solver FPRBVI [21, 22]. The numerical accuracy of both the RKIR and FW–H/RKIR codes will be very similar because the quadrature is based upon the the CFD grid—i.e., all retarded time computations and quadrature points are identical for these two codes. A third code, WOPWOP+ [8], which utilizes the traditional FW–H implementation (surface integration on the blade surface together with an approximate quadrupole implementation) is also used in the comparison. The approximation of the quadrupole integration utilized in WOPWOP+ consists of integrating the Lighthill stress tensor in the direction normal to the rotor plane without regard to retarded time or observer direction. This approximation is essentially exact for a far-field, in-plane observer. The integration volume in the WOPWOP+ calculations is roughly the same as the volume enclosed by the Kirchhoff surface that is utilized in the other codes. (See Refs. 7 and 8 for more details.)

The first comparison is for an untwisted UH-1H model-scale rotor that is operating in hover with a hover tip Mach number $M_H = 0.88$ [23]. Figure 1 shows a comparison of acoustic pressure time history for both the Kirchhoff and FW–H methods on an integration surface that is located approximately 1.37 chordlengths from the rotor in the direction normal to the blade surface and extends 1.25 chordlengths beyond the blade tip. The full-potential computation is performed on an $80 \times 36 \times 24$ grid. Both the full-potential solution and the Kirchhoff computation, along with a description of numerical accuracy, were previously presented by Brentner et al. [5] The grid used here is the coarse grid discussed in Ref. 5. The two acoustic computations are almost indistinguishable in this case—an indication that the integration surface is indeed in the linear flow region. The computer time needed to perform the predictions in Fig. 1 is essentially the same for both the FW–H and Kirchhoff codes. The underprediction of the negative peak is attributable to the coarseness of the CFD grid. Brentner et al. [5] found that the agreement improves with a finer grid. Small oscillations in the signal near the two positive peaks are evident in both the Kirchhoff and FW–H solutions. These oscillations are attributable to inaccurate quadrature over panels that are moving at near-sonic speeds. The wide variation in retarded time over a single panel moving at near-sonic speeds violates the assumption that

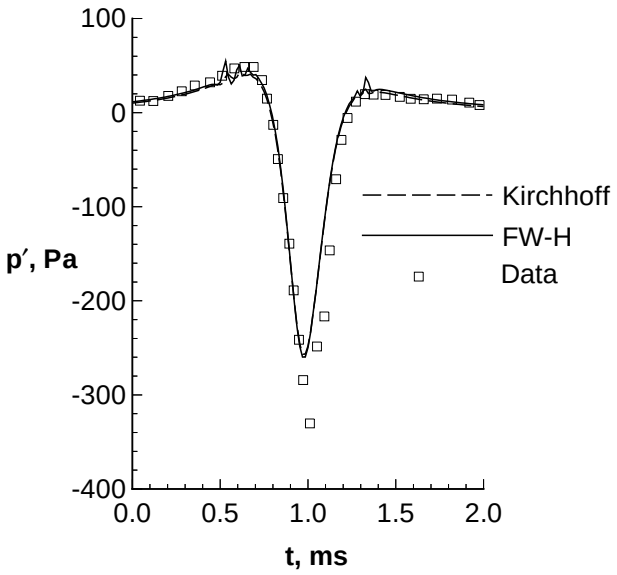

Figure 1. Predicted and measured acoustic pressure at in-plane observer location, $3.09R$ from rotor hub of untwisted UH-1H model rotor in hover at $M_H = 0.88$. (Experimental data are from Ref. 23.)

the integrand is nearly constant over the panel area. The oscillations disappear as the integration surface extent is reduced.

We now examine the sensitivity of each formulation to the placement of the integration surface. Brentner et al. [5] found that the Kirchhoff solution varied depending on the location of the integration surface. Figure 2 shows a cross section of five different integration (Kirchhoff) surface locations that range from 1 grid line off the blade surface to 1.37 chordlengths off the blade surface. The Kirchhoff acoustic pressure predictions from the RKIR code for each of these surface locations are shown in Fig. 3. As the integration surface is brought nearer to the blade surface and the input data are no longer compatible with the wave equation, the predicted acoustic pressure becomes meaningless. Although expected, this aspect of the Kirchhoff method is troublesome. If the integration surface is not positioned properly, the error can be substantial. Furthermore, if the integration surface is positioned even slightly in the nonlinear region, the solution may be significantly in error but not enough so as to be easily recognized.

Figure 4 shows the noise prediction using the FW–H formulation given in Eq. (17) for the same set of integration surfaces and CFD input data as shown in Fig. 3. The volume quadrupole source, which exists only outside the integration surface, has been neglected in this calculation. The advantage of the FW–H formulation is clear: for an integration surface near or on the physical body, the predicted acoustic signal is essentially that of thickness and loading noise alone. As the integration surface is moved farther and farther away, more and more of the quadrupole source contribution is accounted for by the surface integrals. Hence, we would say that the *principal* advantage of the FW–H formulation for aeroacoustics is the relaxation of integration-surface placement restrictions. In fact, when the volume quadrupole source is included in the noise computation, the location of the integration surface is only a matter of choice and convenience.

Another traditional advantage of the FW–H method is the physical basis and identification of the source terms. If Eq. (17) is used on an integration surface away from the body, then this feature is not retained; however, a second computation can be made by integrating over the body surface to determine thickness and loading noise. The results of this second computation are shown in Fig. 5, which presents FW–H/RKIR predictions for comparison with a WOPWOP+ prediction. Two FW–H/RKIR computations are shown in Fig. 5: an integration surface coincident with the rotor blade surface to predict thickness and loading noise and an integration surface located approximately 1.5 chordlengths away from the blade to predict the total noise. Note that the thickness noise predictions from WOPWOP+ and FW–H/RKIR are identical and that only a small difference is evident in the predicted loading noise. The difference in the predicted loading

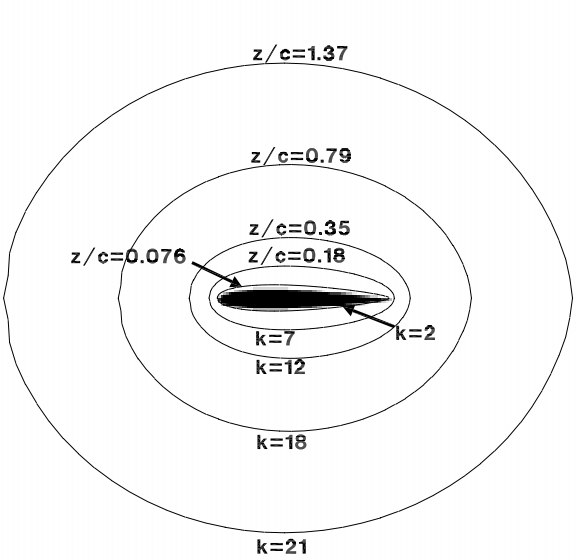

Figure 2. Cross section that shows location of integration surfaces with respect to rotor blade. Vertical distances from blade chord, in units of chord length, are labeled z/c. Value of grid index normal to blade are labeled k.

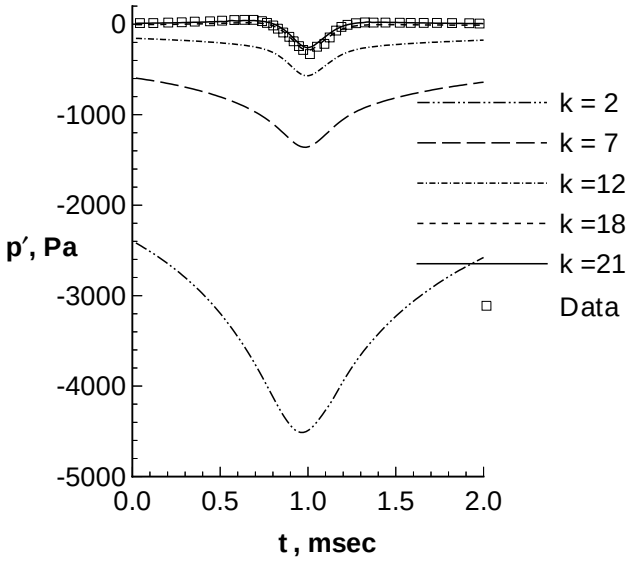

Figure 3. Predicted acoustic pressure using Kirchhoff formulation with varying integration surface locations. Predictions are for in-plane observer located $3.09R$ from UH-1H model rotor in hover at $M_H = 0.88$. (Experimental data are from Ref. 23.)

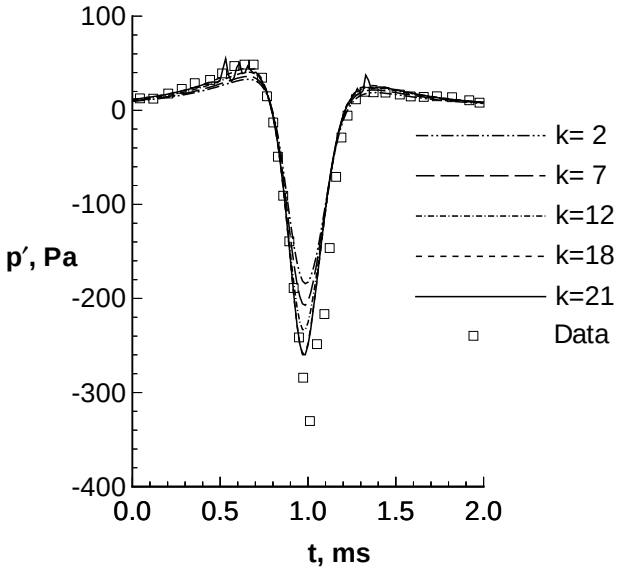

Figure 4. Predicted acoustic pressure using FW–H formulation with varying integration surface locations. Predictions are for in-plane observer located $3.09R$ from UH-1H model rotor in hover at $M_H = 0.88$. (Experimental data are from Ref. 23.)

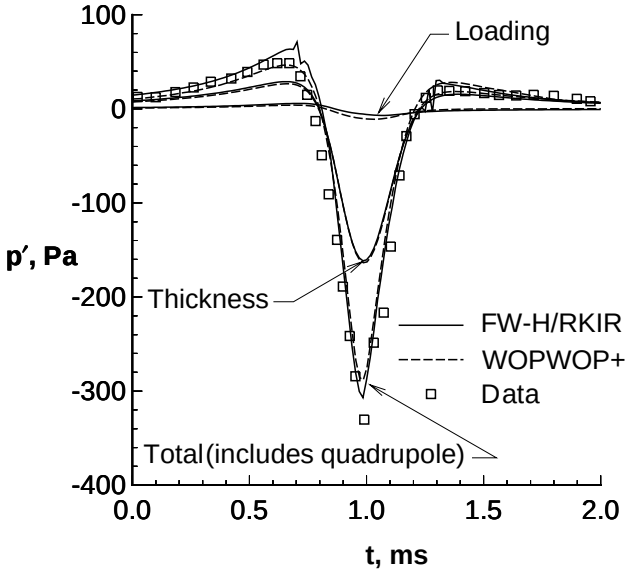

Figure 5. Noise components predicted by FW–H/RKIR and WOPWOP+ codes. Predictions are for in-plane observer located $3.09R$ from UH-1H model rotor in hover at $M_H = 0.88$. (Experimental data are from Ref. 23.)

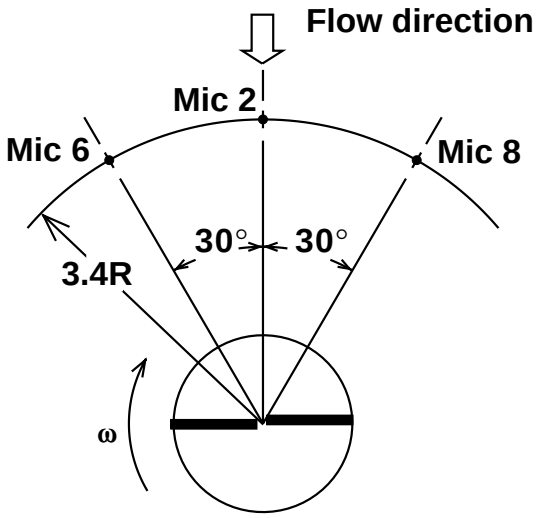

Figure 6. Schematic that shows three in-plane microphone locations used in the measurement of noise from model-scale OLS rotor [24].

noise is attributable to a difference in how the integration over the blade-tip face is handled. The total noise, which includes the effect of the quadrupole, is also in close agreement even though the volume used in WOPWOP+ is not identical to the region enclosed in the FW–H/RKIR surface integration. (The volume integration in the WOPWOP+ calculation is a box shape rather than a cylinder shape.) The negative peak is also in better agreement than in the earlier figures because an Euler solution from Baeder et al. [20] was used as input rather than the FPRBVI solution that was used for Figs. 1, 3, and 4.

A model-scale test of the Operational Loads Survey (OLS) rotor was selected for the final comparison. The predicted noise from the FW–H/RKIR, RKIR, and WOPWOP+ codes is compared with experimental data [24] at three in-plane microphone positions (shown schematically in Fig. 6). The rotor is operating in a forward flight condition with an advancing-tip Mach number $M_{AT} = 0.84$ and an advance ratio $\mu = 0.27$. An FPRBVI full-potential solution is used as input data for the three noise predictions shown in Fig. 7. (The FPRBVI, WOPWOP+, and RKIR predictions were previously described by Brentner et al. [5].) These predictions agree quite well with the data—both in directivity and amplitude. In particular, the codes all predict the correct phase and pulse shape for the three microphone locations. All of the codes underpredict the negative peak pressure for microphone 6, but this result is more likely attributed to the FPRBVI solution rather than the noise prediction codes. The differences between the predictions are most noticeable in the positive peaks, but even in this area the predictions vary by no more than 10 Pa. The FW-H/RKIR and RKIR codes use approximately 20 percent more computational time than WOPWOP+; however, this timing does not include the preprocessing time needed to compute quadrupole source strength.

A New Metric for Comparison

Current CFD convergence criteria are based on the uniform, L_1, or L_2 norms. We propose here that the Sobolev norm is more appropriate as a convergence criterion for high-resolution CFD calculations for both the FW–H and Kirchhoff methods. We hope to stimulate discussion among CFD experts on this point. Although we do not present any numerical results in this paper based on the Sobolev norm, we address the following three questions of interest to aeroacousticians. i) When can a CFD calculation be considered suitably converged so that the data can be used in the acoustic analogy approach? ii) How far from the rotor blade should the permeable surface in the FW–H method be placed to include most of the quadrupole sources? iii) How do we compare two sets of data from converged CFD calculations on a Kirchhoff surface? We attempt to answer these questions in order.

We assume that the CFD code used to supply fluid mechanic data for acoustic calculations is based on a consistent and stable scheme [25, 26]. We also assume that a grid size study has been performed and a

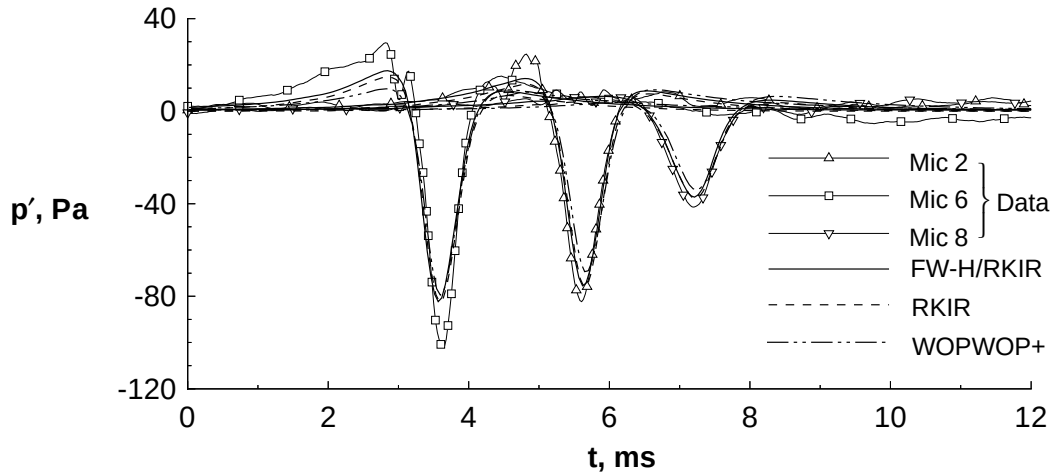

Figure 7. Predicted and measured acoustic pressure at three microphone locations for model-scale OLS rotor ($M_{AT} = 0.84;\ \mu = 0.27$). (Experimental data are from Ref. 24.)

satisfactory spatial and temporal grid sizes have been selected. Below the Sobolev norms that we propose are written for a smooth function. In practice, however, the integrals and the derivatives must be written in finite difference form based on the values of the functions involved in the definition of the norm on the grid points. Since we are always dealing with time-dependent CFD calculations, we use the term iteration when we mean subiteration for convergence of the scheme at a given time.

i) CFD Convergence

We note that the solution of the FW–H equation with the quadrupole source term invariably involves the Lighthill stress tensor T_{ij} and its first and second derivatives. Therefore, it is imperative that not only T_{ij} is calculated accurately but also its first and second derivatives in the source region. This suggests that the error analysis in high-resolution CFD computations must be based on the Sobolev norm. This norm is used quite often in finite-element analysis [27], and we propose such a norm in aeroacoustics. We define two Sobolev norms of T_{ij} as follows;

$$\|T_{ij}\|_V^{(1)} = \Big[\int_0^T \int_V \Big(\sum_{i,j} |T_{ij}|^2 + \sum_j \Big|\frac{\partial T_{ij}}{\partial x_i}\Big|^2 + \Big|\frac{\partial^2 T_{ij}}{\partial x_i \partial x_j}\Big|^2\Big) d\mathbf{x}\ dt\Big]^{1/2}, \tag{19a}$$

$$\|T_{ij}\|_V^{(2)} = \max_{t\epsilon[0,T]} \Big[\int_V \Big(\sum_{i,j} |T_{ij}|^2 + \sum_j \Big|\frac{\partial T_{ij}}{\partial x_i}\Big|^2 + \Big|\frac{\partial^2 T_{ij}}{\partial x_i \partial x_j}\Big|^2\Big) d\mathbf{x}\Big]^{1/2} \tag{19b}$$

where T_{ij} and its derivatives are given in nondimensional form and T is a convenient time period. We propose that T be taken as the inverse of the blade passage frequency. Here, V is the volume of the CFD calculation. Thus, we have a metric for a convergence criterion for evaluating CFD calculations. We define the distance between two CFD results as

$$d(T_{ij}^1, T_{ij}^2)^{(i)} = \|T_{ij}^1 - T_{ij}^2\|_V^{(i)} \qquad (i = 1 \text{ or } 2). \tag{20}$$

The convergence criterion in an iterative CFD code should be based on

$$d(T_{ij}^{n+1}, T_{ij}^n)^{(i)} = \|T_{ij}^{n+1} - T_{ij}^n\|_V^{(i)} \to 0 \qquad (i = 1 \text{ or } 2). \tag{21}$$

where the superscripts n and $n+1$ stand for the CFD results at the nth and $(n+1)$th iteration.

ii) Integration Surface Placement

An alternate use of the norm defined in Eq. (19) is to determine the volume of quadrupole sources to be included in the noise calculation. We assume that the CFD results have converged based on one of the Sobolev norms defined in Eq. (19). Let V_1 and V_2 be two volumes, with boundaries ∂V_1 and ∂V_2, such that $V_1 \subset V_2$. Then, assume that $T_{ij}^1 = 0$ outside V_1. By using the Sobolev norm with volume integration over V_2, we can say that V_2 includes all quadrupoles needed for the noise calculation if

$$\frac{\left\| T_{ij}^1 - T_{ij}^2 \right\|_{V_2}^{(i)}}{\left\| T_{ij}^1 \right\|_{V_1}} \ll 1 \qquad (i = 1 \text{ or } 2) \ . \tag{22}$$

Thus,

$$\left\| T_{ij}^2 \right\|_{V_2 \setminus V_1}^{(i)} \ll \left\| T_{ij}^1 \right\|_{V_1}^{(i)} \qquad (i = 1 \text{ or } 2) \tag{23}$$

where $V_2 \setminus V_1$ is the volume enclosed between ∂V_1 and ∂V_2. This answers the question of how far from the blade surface we must include the quadrupole sources.

iii) Comparison of Kirchhoff Data

Similarly, the Kirchhoff formula tells us that, on the Kirchhoff surface, p', $\dot{p}'$, and $\partial p'/\partial n \equiv p'_n$ must be computed accurately in the CFD solution. Assume that S is the Kirchhoff surface over which the nondimensional p', $\dot{p}'$, and p'_n are specified. We define two Sobolev norms of p' and the distance between two CFD solutions p'^1 and p'^2 as follows:

$$\left\| p' \right\|_S^{(1)} = \left\{ \int_0^T \int_S \left[|p'|^2 + \ |\dot{p}'|^2 + |p'_n|^2 \right] dS dt \right\}^{1/2} , \tag{24a}$$

$$\left\| p' \right\|_S^{(2)} = \max_{t \epsilon [0,T]} \left\{ \int_S \left[|p'|^2 + \ |\dot{p}'|^2 + |p'_n|^2 \right] dS \right\}^{1/2} , \tag{24b}$$

and

$$d(p'^1, p'^2)^{(i)} = \left\| p'^1 - p'^2 \right\|_S^{(i)} \tag{25}$$

where p'^1 and p'^2 are two sets of acoustic pressure data on S. Now we assume that we have two sets of CFD results from converged solutions based on *any* norm used for the CFD convergence criterion. We want to know whether these solutions will yield similar acoustic results when used with the Kirchhoff formula. The answer lies in the following inequality:

$$\frac{\left\| p'^1 - p'^2 \right\|_S^{(i)}}{\left\| p'^1 \right\|_S^{(i)}} \ll 1 \tag{26}$$

Note that this inequality can only be used to evaluate how "close" two sets of data on a Kirchhoff surface are (i.e., in terms of the resulting acoustic prediction); the accuracy of either set of data cannot be evaluated. This latter question can only be answered by the convergence of the CFD based on either of the Sobolev norms defined in Eq. (19). We believe that the calculation of the Sobolev norm in current CFD codes is feasible without undue difficulty.

Conclusions

In this paper, we have compared two useful aeroacoustic tools: the Lighthill acoustic analogy as embodied in the Ffowcs Williams–Hawkings (FW–H) equation and the Kirchhoff formulation for moving surfaces. Both methodologies have proven their usefulness in rotor noise prediction. Because both methods work well, deciding which method to use for a particular application can be difficult. In a comparison of the

governing equations, we have shown that the FW–H approach can include nonlinear flow effects in the surface integration if the usual assumption of an impenetrable surface is relaxed. In fact, we have shown that the FW–H equation is equivalent to the Kirchhoff governing equation when the integration surface is located in the linear flow region.

The FW–H equation is based on the conservation laws of fluid mechanics rather than on the wave equation, which is the case for the Kirchhoff formula. Consequently, the FW–H equation is not appropriate for all types of wave propagation. (For example, the FW–H equation is not appropriate for electromagnetic wave propagation, but the Kirchhoff formula could be utilized.) However, the superiority of the FW–H approach for the aeroacoustics of rotating blades has been demonstrated in several numerical examples in this paper. The placement of the integration surface for the FW–H method is a matter of convenience as long as the quadrupole source is utilized. The FW–H method also has an advantage in that the predicted noise is explicitly separated into physical components (i.e., thickness, loading, and quadrupole). The Kirchhoff method does not offer this insight into the acoustic field. These advantages of the FW–H approach can be realized with essentially no increase in computational effort.

It is well known that the quadrupole sources are responsible for noise generation as well as distortion of the acoustic waveform. The calculations in this paper and those of di Francescantonio [11] demonstrate that the surface source terms of the FW–H equation account for the nonlinear quadrupole sources surrounded by a permeable integration surface. The most intense quadrupole sources are in the vicinity of the blades. Therefore, if we use a surface that encloses the blade and the volume of intense quadrupoles in the FW–H method, then we can accurately calculate the level of acoustic pressure. The role of the weaker quadrupoles, which are farther away from the physical body, is primarily to provide a small distortion to the acoustic waveform. Hence, even when the integration surface is fairly close to the noise generating surface, the external quadrupoles may be neglected. In comparison, with the Kirchhoff formula the predicted acoustic pressures can be substantially in error if the Kirchhoff surface is positioned inside the nonlinear region; the nature and order of magnitude of this error may be hard to estimate or even recognize.

In summary, the results presented in this paper lead us to conclude that the FW–H approach is unquestionably superior to the Kirchhoff method for aeroacoustic problems because 1) the governing equations for the FW–H approach contain full knowledge of the conservation of mass and momentum for the fluid yet are equivalent to the Kirchhoff formulation the linear region; 2) the FW–H approach is more robust— the integration surface can be placed anywhere if the quadrupole source is included, and the FW–H solution is less sensitive to placement of the integration surface if the quadrupole is neglected; 3) the FW–H approach offers physical insight into the sound-generation process; and 4) essentially no increase in computational effort is associated with the FW–H method as compared with the Kirchhoff method when the quadrupole source is neglected.

REFERENCES

1. Lighthill, M. J., "On Sound Generated Aerodynamically, I: General Theory," *Proceedings of the Royal Society*, Vol. A211, 1952, pp. 564–587.

2. Ffowcs Williams, J. E., and Hawkings, D. L., "Sound Generated by Turbulence and Surfaces in Arbitrary Motion," *Philosophical Transactions of the Royal Society*, Vol. A264, No. 1151, 1969, pp. 321–342.

3. Farassat, F., and Myers, M. K., "Extension of Kirchhoff's Formula to Radiation from Moving Surfaces," *Journal of Sound and Vibration*, Vol. 123, No. 3, 1988, pp. 451–461.

4. Farassat, F., and Myers, M. K., "The Kirchhoff Formula for a Supersonically Moving Surface," *Proceedings of the 1st Joint CEAS / AIAA Aeroacoustics Conference (16th AIAA Aeroacoustics Conference)*, Vol. I, 1995, pp. 455–463. CEAS/AIAA Paper 95-062.

5. Brentner, K. S., Lyrintzis, A. S., and Koutsavdis, E. K., "Comparison of Computational Aeroacoustic Prediction Methods for Transonic Rotor Noise Prediction," *Journal of Aircraft*, Vol. 34, No. 4, July-Aug. 1997, pp. 531–538.

6. Brentner, K. S., "Prediction of Helicopter Discrete Frequency Rotor Noise—A Computer Program Incorporating Realistic Blade Motions and Advanced Formulation," NASA TM 87721, Oct. 1986.

7. Brentner, K. S., and Holland, P. C., "An Efficient and Robust Method for Computing Quadrupole Noise," *Journal of the American Helicopter Society*, Vol. 42, No. 2, Apr. 1997, pp. 172–181.

8. Brentner, K. S., "An Efficient and Robust Method for Predicting Helicopter Rotor High-Speed Impulsive Noise," *Journal of Sound and Vibration*, Vol. 203, No. 1, 1997.

9. Xue, Y., and Lyrintzis, A. S., "Rotating Kirchhoff Method for Three-Dimensional Transonic Blade-Vortex Interaction Hover Noise," *AIAA Journal*, Vol. 32, No. 7, July 1994, pp. 1350–1359.

10. Lyrintzis, A. S., Koutsavdis, E. K., Berezin, C., Visintainer, J., and Pollack, M., "Kirchhoff Acoustic Methodology Validation and Implementation in the TiltRotor Aeroacoustic Codes (TRAC)," American Helicopter Society 2nd International Aeromechanics Specialists' Conference, Oct. 1995.

11. di Francescantonio, P., "A New Boundary Integral Formulation for the Prediction of Sound Radiation," *Journal of Sound and Vibration*, Vol. 202, No. 4, 1997, pp. 491–509.

12. Pilon, A. R., and Lyrintzis, A. S., "Integral Methods for Computational Aeroacoustics," AIAA Paper 97-0020, Jan. 1997.

13. Farassat, F., "Quadrupole Source in Prediction of Noise of Rotating Blades—A New Source Description," AIAA Paper 87-2675, 1987.

14. Farassat, F., and Brentner, K. S., "The Uses and Abuses of the Acoustic Analogy in Helicopter Rotor Noise Prediction," *Journal of the American Helicopter Society*, Vol. 33, No. 1, Jan. 1988, pp. 29–36.

15. Farassat, F., and Myers, M. K., "An Analysis of the Quadrupole Noise Source of High Speed Rotating Blades," *Computational Acoustics—Scattering, Gaussian Beams, and Aeroacoustics*, edited by D. Lee, A. Cakmak, and R. Vichnevetsky, North-Holland, Amsterdam, Vol. 2, 1990, pp. 227–240.

16. Farassat, F., "Introduction to Generalized Functions With Applications in Aerodynamics and Aeroacoustics," NASA TP 3428, May 1994. See corrected version, April 1996. Available online at ftp://techreports.larc.nasa.gov/pub/techreports/larc/94/tp3428.ps.Z directly.

17. Dowling, A. P., and Ffowcs Williams, J. E., *Sound and Sources of Sound*, Ellis Horwood Publishers, Chichester, West Sussex, England, 1983.

18. Crighton, D. G., Dowling, A. P., Ffowcs Williams, J. E., Heckl, M., and Leppington, F. G., *Modern Methods in Analytical Acoustics: Lecture Notes*, Springer-Verlag, London, 1992.

19. Farassat, F., and Succi, G. P., "The Prediction of Helicopter Discrete Frequency Noise," *Vertica*, Vol. 7, No. 4, 1983, pp. 309–320.

20. Baeder, J. D., Gallman, J. M., and Yu, Y. H., "A Computational Study of Aeroacoustics of Rotors in Hover," *Journal of the American Helicopter Society*, Vol. 42, No. 1, Jan. 1997, pp. 39–53.

21. Burley, C. L., and Tadghighi, H., "Importance of High Accuracy Blade Motion and Airloads Predictions in Acoustic Analysis," American Helicopter Society 50th Annual Forum, 1994.

22. Prichard, D. S., Boyd, Jr., D. D., and Burley, C. L., "NASA Langley's CFD–Based BVI Rotor Noise Prediction System: (ROTONET/FPRBVI) An Introduction and User's Guide," NASA TM 109147, Nov. 1994.

23. Purcell, T. W., "CFD and Transonic Helicopter Sound," Fourteenth European Rotorcraft Forum, 1988. Paper 2.

24. Schmitz, F. H., Boxwell, D. A., Splettstoesser, W. R., and Schultz, K. J., "Model-Rotor High-Speed Impulsive Noise: Full-Scale Comparisons and Parametric Variations," *Vertica*, Vol. 8, No. 4, 1984, pp. 395–422.

25. Richtmyer, R. D., and Morton, K. W., *Difference Methods for Initial-Value Problems*, Interscience Publisher, Inc., New York, 2nd edition, 1967.

26. Tannehill, J. C., Anderson, D. A., and Pletcher, R. H., *Computational Fluid Mechanics and Heat Transfer*, Taylor and Francis Publishers, Washington, D.C., 2nd edition, 1997.

27. Brenner, S. C., and Scott, C. R., *The Mathematical Theory of Finite Element Methods*, Springer-Verlag, New York, 1994.